Journal of Statistical Physics, Vol. 74, Nos. 5/6, 1994

The Domany–Kinzel Cellular Automaton Phase Diagram

G. F. Zebende[1] and T. J. P. Penna[1]

Received July 20, 1993

The boundaries between the three phases of the Domany–Kinzel probabilistic cellular automaton are determined with high accuracy via the gradient method. The difficulties the extrapolation to the thermodynamic limit are circumvented and the critical exponents are also presented.

KEY WORDS: Cellular automata; damage spreading; phase transitions.

Cellular automata (CA) are discrete dynamical systems that find wide and general applications in science.[1,2] Since the dynamics is not restricted to the usual Boltzmann weight and detailed balance, CA have been used to model out-of-equilibrium processes, and even one-dimensional CA can present complex behavior such as continuous phase transitions with critical exponents. The local rules of a CA can be deterministic or, in a more general case, probabilistic (PCA). A very interesting PCA is the so-called Domany–Kinzel PCA.[3] The probabilistic cellular automaton studied by Domany and Kinzel consists of a linear chain of N sites ($i = 1, 2, ..., N$). Each site may be in one of two states, $\sigma_i = 0, 1$ (empty, occupied). The sites are updated in parallel at discrete time steps according to the conditional probabilities $\{P(\sigma_{i-1}(t), \sigma_{i+1}(t) \mid \sigma_i(t+1))\}$, i.e., the state of a site at given time $t+1$ will depend upon the state of the two nearest-neighbor sites at time t. In the isotropic case $P(0, 1 \mid 1) = P(1, 0 \mid 1) = p1$, $P(1, 1 \mid 1) = p2$, and $P(0, 0 \mid 1) = 0$.

The phase diagram of the Domany–Kinzel PCA presents three different phases depending on the values of $(p1, p2)$. In the first phase, the asymptotic state is homogeneous with all sites set to 0 (*frozen phase*). If the

[1] Instituto de Física, Universidade Federal Fluminense, C.P. 100296, 24001-970, Niterói, RJ, Brazil. e-mail: Gfitjpp@BRUFF.bitnet.

0022-4715/94/0300-1273$07.00/0

values of $p1$ and $p2$ are increased the asymptotic state has a finite fraction of interchanging sites set to 1 (*active phase*). This phase transition was demonstrated by Domany and Kinzel[3] based on results from transfer matrix equations. Recently, Martins *et al.*[4] by performing numerical simulations with systems up to $N=3200$, found that the active phase can be split into two phases, called chaotic and nonchaotic, where the order parameter is the distance between two different configurations (damage). Via larger numerical simulations ($N>10^4$ sites), Kohring and Schreckenberg[5] pointed out the difficulties in extrapolating the results from simulations to the thermodynamic limit due to the unusual finite-size effects, namely, the order parameters are not monotonic functions of the system size. Kohring and Schreckenberg studied numerically only the behavior in the line $p2=0$, a region where the paper of Domany and Kinzel is ambiguous. The results available do not rule out the existence of a critical point $p2\neq 0$, since numerical simulations close to $p2=0$ were not performed in refs. 4 and 5. The analytical results from ref. 5 show a tricritical point located at $p2=1$ in a mean field approximation and at $p2=0$ using one step beyond (two-tree approximation).[6]

In this work we used both the gradient[7] and damage spreading in a gradient[8] techniques to determine, with high accuracy, the phase diagram of the Domany–Kinzel PCA. These techniques were applied to determine the critical points of percolation,[7] the Kauffman model and the XOR-OR mixture,[8] and thermal phase transitions in ferromagnetic and spin-glass models.[9,10] In order to apply that technique to the Domany–Kinzel PCA, we adopted the time as second dimension (y direction, for instance), i.e., we stored $L_\perp$ steps in the time evolution of the system and we constructed a lattice with dimensions $N\times L_\perp$. Different strategies were adopted to study the two boundaries. Let us concentrate first on the frozen–active transition. For a given value of $p2$, each line of fixed x direction has a different value of $p1$. The site on the left boundary is fixed to zero and the state of one in the right boundary is set at random. The probability $p1$ for the jth site will be

$$p1(j)=p1(1)+\frac{p1(N)-p1(1)}{N-1}(j-1) \tag{1}$$

We chose $p1(1)<p1_c$ and $p1(N)>p1_c$. Only a rough estimative of $p1_c$ is needed at this stage. The site on the left (right) boundary was considered as the zeroth [$(N+1)$th] site. Typically we worked with a small $N=640$ lattice. The results are almost insensitive to the dimension N. We found the same results within the error bars for different N; therefore we choose $N=640$ for the time saving (for smaller lattices the cluster of frozen sites

touches the boundaries frequently). In this strategy the thermodynamic limit is extrapolated by making the gradient

$$\nabla = [p1(N) - p1(1)]/N \tag{2}$$

go to zero. After waiting many time steps (10,000 in this work) we start to store the time evolution of the system. We measure both the number of sites belonging to this cluster and those that define the front of the cluster (this cluster is a compact one). From these quantities we can determine the critical point and the exponents.[8,9] The density $\rho(j)$ of frozen sites per line is shown in Fig. 1 for three different values of ∇. Using the scaling law proposed by da Silva and Herrmann,[8]

$$\rho(p1) = (\nabla p1)^x \mathscr{F}[(p1 - p1_c)(\nabla p1)^{-y}] \tag{3}$$

where $\mathscr{F}$ is a scaling function, one could extract the critical exponent $\beta = x/y$ and the transition point from the frozen to the active phase. Figure 2 shows the data collapse for the parameters $x = 0.19 \pm 0.01$, $y = 0.79 \pm 0.01$, and $p1_c = 0.675 \pm 0.008$. The value found for $\beta = 0.24 \pm 0.02$ agrees well with the one found by Martins *et al.*, $\beta = 0.25 \pm 0.02$. A more precise way to obtain the critical boundary is via the average position p_m of the boundary of the frozen cluster.[8] After the thermalization, p_m evaluated from $L_\perp$ time steps differs less than 0.01% from the $L_\perp/2$. We used $L_\perp = 3000$ in our simulations. Figure 3 show p_m as a function of ∇ for different $p2$. From this plot we can estimate the value of $p1_c$ in the thermodynamical limit, extrapolating to $\nabla = 0$. For the limit cases $p2 = 0$ (1)

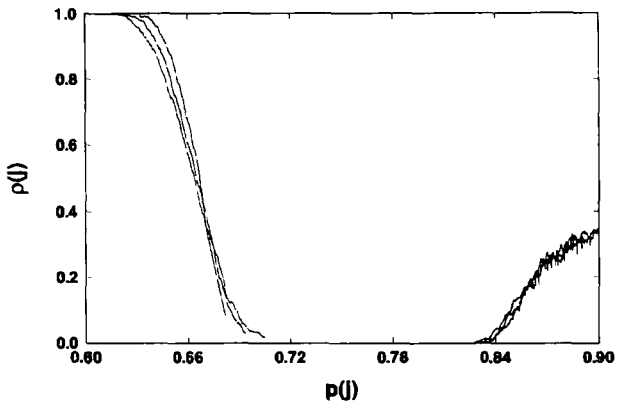

Fig. 1. Plot of $\rho(j)$ (frozen cluster at left and damaged cluster at right) as a function of $pi(j)$ ($i = 1$ for the frozen cluster and $i = 2$ for the damaged one).

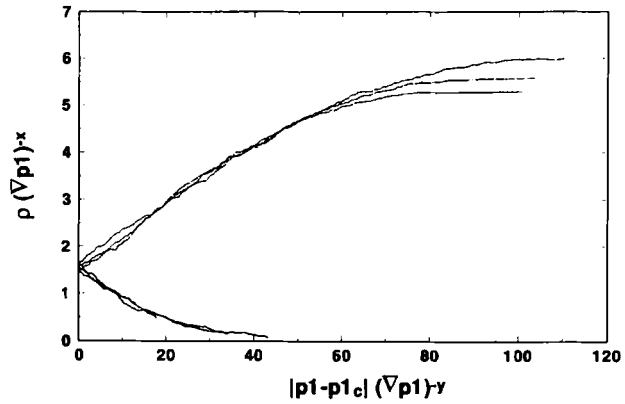

Fig. 2. Scaling plot for the parameters $x = 0.19$, $y = 0.8$, and $p1_c = 0.675$ ($p2 = 0.8$).

[$p1_c = 0.799 \pm 0.002$ (0.496 ± 0.005)], the agreement is excellent with the previous results $p1_c = 0.8$ (0.5).[3-5] The phase diagram presented in Fig. 4 is to be compared to the original results of Martins *et al.*[4] The shape of the frozen–active boundary from this work is more similar to the one found by transfer matrix equations.[3] The shift in the critical boundary for intermediate values of $p2$ compared to the one found in ref. 4 can be explained by finite-size and time effects. Larger simulations have seen this displacement for $p2 = 0.5$.[11] The shift is smaller close to the deterministic $p2$ values, as we can expect due to stochastic effects, which are more important close to $p2 = 0.5$ (there is no shift for the limit cases $p2 = 0$ (1)).

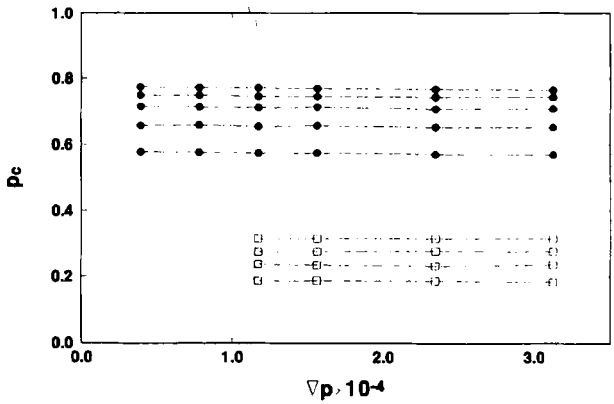

Fig. 3. Average p_c as function of ∇p for different $p2$ for the frozen–active (●) and the active–chaotic transitions (□).

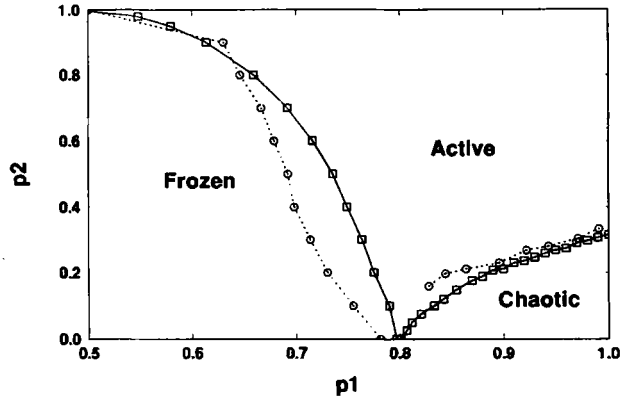

Fig. 4. Phase diagram of the Domany–Kinzel PCA: ○ and dotted lines, Martins *et al.*; □ and full lines, this work.

In order to check if this range of gradients corresponds to a region where finite-size effects are not so relevant, we performed simulations for three different sizes ($N = 320$, 640, and 1024 sites). The results are shown in Fig. 5 and we can conclude that in this region finite-size effects do not seem to be important. The extrapolated values are $p_c = 0.834(3)$, 0.832(2), and 0.833(3) for $N = 320$, 640, and 1024, respectively. These sizes are larger than the ones that present anomalous behavior.[5] We also tested the method using an orthogonal gradient, i.e., $p1$ is kept fixed and the gradient is performed in the $p2$. The agreement is found within 0.1%, corroborating the high accuracy of our results.

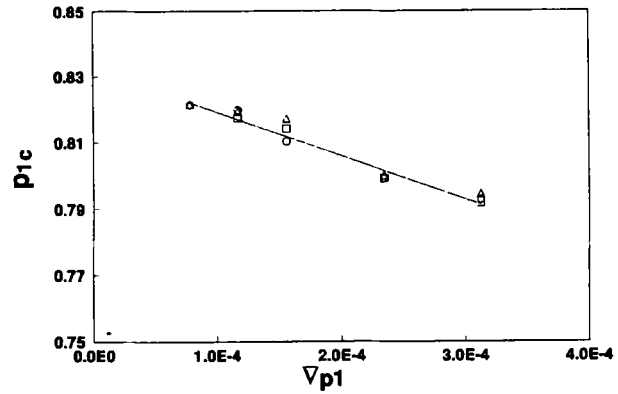

Fig. 5. Plot of $p1_c$ as a function of $\nabla p1$ for three different sizes, $N = 320$ (△), 640 (□), and 1024 (○). The solid line is a regression evaluated over the $N = 640$ data ($p2 = 0.1$).

We repeat the same procedure for the active–chaotic phase. For this case we studied the time evolution of two configurations that differ initially by only one site. This damage is kept during the evolution, i.e., these sites are not updated. The differences compared to frozen–active boundaries are: the damaged cluster is no longer compact, although we can still define the average position $p1_c$ of the damage boundary; and we had to systemize the orientation of the gradients: close to the $p2 = 0$ line the gradient is applied to $p1$ and close to the $p1 = 1$ the gradient is applied to $p2$. The damage cluster is not compact, so the determination of the exponents is not precise as in the frozen–active transition (see Fig. 1). The critical exponent of the order parameter Ψ (damage per site) found was $\mu = 0.37 \pm 0.05$ and agrees very well with the one found by Martins *et al.*[4] The tricritical point is located at ($p1 = 0.801 \pm 0.002$, $p2 = 0$). The other marginal point is located at ($p1 = 1$, $p2 = 0.3147 \pm 0.0002$). We can note a shift compared to ref. 4 also in this transition and we attribute this result also to finite-size effects. The active–chaotic boundary is a monotonic function of $p1$ as found in ref. 4 and opposite to what is suggested by analytical results in ref. 5.

We have studied the frozen and damage boundaries into a gradient. The average concentration p_m for both transitions is determined with quite precise values ($\approx 0.1\%$) even for small lattices. With this powerful method we can obtain the complete phase diagram, overcoming the difficulties pointed out by Kohring and Schreckenberg. Our simulations were carried out on Sun SPARC 2 workstations. For an $N = 640$ lattice, our multispin code updates 170×10^3 sites/sec.

ACKNOWLEDGMENTS

This work is partially supported by Brazilian agencies CAPES and CNPq. The authors are indebted to C. Tsallis, M. L. Martins, P. M. C. de Oliveira, and L. R. Silva for discussions.

REFERENCES

1. S. Wolfram, *Theory and Applications of Cellular Automata* (World Scientific, Singapore, 1986).
2. D. Stauffer, *J. Phys. A* **24**:909 (1991).
3. E. Domany and W. Kinzel, *Phys. Rev. Lett.* **53**:311 (1984); W. Kinzel, *Z. Phys. B* **58**:229 (1985).
4. M. L. Martins, H. F. Verona de Rezende, C. Tsallis, and A. C. N. de Magalhães, *Phys. Rev. Lett.* **66**:2045 (1991).

5. G. A. Kohring and M. Schreckenberg, *J. Phys. I* (Paris) **2**:2033 (1992).
6. J. Cook and B. Derrida, *J. Phys. A* **23**:1523 (1990).
7. B. Sapoval, M. Rosso, and J.-F. Gouyet, *J. Phys. Lett.* (Paris) **46**:L749 (1985).
8. L. R. da Silva and H. J. Herrmann, *J. Stat. Phys.* **52**:463 (1988).
9. N. Boissin and H. J. Herrmann, *J. Phys. A* **24**:L43 (1991).
10. G. G. Batrouni and A. Hansen, *J. Phys. A* **25**:L1059 (1992).
11. M. L. Martins, G. F. Zebende, T. J. P. Penna, and C. Tsallis, preprint (1993).

Communicated by D. Stauffer